FISEVIER

Contents lists available at ScienceDirect

# **Energy for Sustainable Development**



# The effects of modified operation on emissions from a pellet-fed, forced-draft gasifier stove



Stephanie Parsons, Ky Tanner <sup>1</sup>, Wyatt Champion <sup>2</sup>, Andrew Grieshop \*

Department of Civil, Construction, and Environmental Engineering, North Carolina State University, Raleigh, NC 27695, United States

#### ARTICLE INFO

Article history:
Received 31 March 2022
Revised 21 July 2022
Accepted 2 August 2022
Available online 12 August 2022

Keywords:
Cookstove emissions
Gasifier cookstoves
Emission rate
Particle size distribution

#### ABSTRACT

Traditional solid fuel cookstoves emit gas- and particle-phase pollutants that contribute to household air pollution, human disease, and climate impacts. Forced-draft semi-gasifier stoves are an attractive intermediate step to zero-emitting stoves due to their reported lower emissions in laboratory and field studies, and potential for increased availability in more rural locales. However, emissions from these stoves have been shown to be highly variable and sensitive to stove design, fuel type, secondary air velocity, and operation mode. We measured carbon monoxide (CO), particulate matter (PM<sub>2.5</sub>), organic and elemental carbon, and particle number (15–685 nm) emissions of the widely adopted Mimi Moto pellet-fed, gasifier stove for different operating conditions under two modified protocols, the Water Boiling Test (WBT) and an updated laboratory testing protocol ISO 19867-1 (ISO). We categorized operating conditions into three approaches: Startup (varying ignition material), Shutdown (varying fan speed during a 45-min burnout period), and Refuel (varying the height of charred pellets added for re-ignition). Refueling led to the largest and most variable emissions, but lab emissions were all lower than high field emissions (e.g., similar to those of traditional solid fuels) and remained primarily in ISO Tiers 5 and 4 for CO and PM2.5, aspirational and second-best, respectively. We find large relative differences in emissions when comparing our results to similar studies conducted with the Mimi Moto and ISO protocol, suggesting small operational differences can have large emissions implications. To minimize emissions, we recommend using kerosene for ignition, turning the fan off when pellets are done burning and flame has extinguished, and reigniting with fresh pellets instead of pellet char. Improved training and maintenance are needed in realworld applications to decrease the frequency of high-emission events. Tightly constrained testing and detection limits remain challenges to fully understanding factors contributing to these events.

#### Introduction

Around three billion people cook using open fires or simple kerosene, biomass, and coal stoves, contributing to 2.2 million premature deaths from illnesses attributable to household air pollution, such as chronic obstructive pulmonary disease and stroke (Health Effects Institute, 2020; Rehfuess et al., 2006; Smith et al., 2004). Pollutants contributing to these illnesses are mainly products of incomplete combustion emitted by solid fuel combustion and include both gas- and

particle-phase components. Gaseous pollutants emitted include carbon monoxide (CO), carbon dioxide (CO<sub>2</sub>), methane, nitrogen oxides (NO<sub>x</sub>), and hydrocarbons, which affect the respiratory and cardiovascular systems (Kampa & Castanas, 2008; Rosenthal, 2015). CO in particular is known to cause impaired neurocognitive ability such as loss of concentration, dizziness, and confusion (Raub & Benignus, 2002; US Department of Health and Human Services, 2012; Wilbur et al., 2012).

Particulate matter (PM) varies widely in size, and its characterization is crucial to understanding both health and climate impacts of household air pollution (Bell et al., 2007; Health Effects Institute, 2020; Smith et al., 2014). PM<sub>2.5</sub> denotes particles with aerodynamic diameters <2.5  $\mu$ m, while ultrafine particles (UFPs defined here as PM<sub>0.1</sub>) are particles with diameters <0.1  $\mu$ m (US EPA, 2019). Particle number emissions and size distributions are key factors for determining lung deposition and subsequently influence particle health effects (Vu et al., 2015). Studies have reported worse health effects when considering number of UFPs compared to mass of PM<sub>2.5</sub> as UFPs can travel deeper into the lung, have more surface area per mass (i.e., enhanced chemistry and bioavailability),

<sup>\*</sup> Corresponding author at: Department of Civil, Construction, and Environmental Engineering, North Carolina State University, 3165 Fitts-Woolard Hall, 915 Partners Way, Raleigh, NC 27695-7908, United States.

<sup>&</sup>lt;sup>1</sup> Current affiliation: Department of Mechanical Engineering, Colorado State University, Fort Collins, Colorado, 80523, United States.

<sup>&</sup>lt;sup>2</sup> Current affiliation: Jacobs Technology Inc., 600 William Northern Boulevard, Tullahoma, Tennessee 37388, United States.

and can even penetrate into the bloodstream allowing translocation to other organ systems (Li et al., 2003; Peters et al., 1997; Schraufnagel, 2020).

Certain emitted pollutants, such as greenhouse gases (e.g., CO<sub>2</sub>, methane), have long atmospheric lifetimes and contribute to the warming of Earth's climate. PM also affects climate by scattering and/ or absorbing solar radiation, changing cloud radiative properties, and influencing atmospheric chemistry (Meyer et al., 2015; Eilenberg et al., 2018). Two important components of PM<sub>2.5</sub> in terms of global warming are organic and elemental carbon (OC, EC) due to their strong scattering and absorption properties, respectively (IPCC, 2021). The direct radiative effect of most aerosols is cooling due to scattering of solar radiation; however, absorbing aerosols, such as black carbon (BC) can warm the atmosphere via absorption (Meyer et al., 2015; Ramanathan et al., 2001). Biomass fuels (wood, agricultural waste, dung, and coal) used for cooking contribute approximately 25 % of global BC emissions, which absorb solar radiation and leads to atmospheric warming (Bond et al., 2013; Lacey et al., 2017). The health and climate impacts of existing and alternative biomass combustion technologies are thus affected by multiple properties of gas- and particlephase emissions, and therefore warrant careful study.

Various fuel and stove combinations have been developed and explored to address the impacts of solid fuel combustion. While the ideal is a fully renewable and zero-emitting stove/fuel combination, cleanerburning alternative solid fuel stoves may provide an intermediate step, especially for rural populations where transitions to liquified petroleum gas (LPG) or electricity may be less feasible. Forced-draft semi-gasifier stoves are attractive due to lower emission measurements reported in laboratory (Bilsback et al., 2018; Carter et al., 2014; Chen et al., 2016; Jetter et al., 2012; Jetter & Kariher, 2009; Li et al., 2016; Shen, 2016; Tryner et al., 2016) and field studies (Garland et al., 2017; Sandro et al., 2019; Shan et al., 2017; Shen et al., 2012). Champion and Grieshop (2019) measured CO, PM<sub>2.5</sub>, EC, and BC emissions from pellet-fed forced-draft gasifier, wood, and charcoal stoves in 91 uncontrolled cooking tests in urban Rwanda and found in-use pellet gasifier stoves to have climate and health benefits approaching that of LPG (Champion & Grieshop, 2019).

Forced-draft semi-gasifier stoves (sometimes referred to as toplit updraft, or TLUD) use fuel batch-fed into a combustion chamber, ignited from the top, and burned top down. A fan supplies primary air into the base of the combustion chamber and secondary air above the fuel bed. Primary air converts the fuel to a hot and combustible gas (i.e., devolatilization) while secondary air is preheated by the walls of the chamber and mixed with the combustible gas in the chamber via secondary air inlet holes (Reed & Larson, 1996). This two-stage combustion process enables better mixing of the gases with air and thus more complete combustion (Anderson et al., 2007). However, because the fan pushes relatively cool air into the combustion chamber, low temperature regions may form, inhibiting oxidation and promoting organic vapor condensation (Turns, 2012). Additionally, the higher density and homogeneity of biomass pellets (as well as relatively uniform flame front) improve combustion compared to that of larger, unprocessed fuel such as splintered wood or charcoal (Champion et al., 2020; Zhou et al., 2016). While bulk density within the chamber is dependent on pellet alignment, Gutiérrez et al. (2022) investigated biomass bulk density of pellets and wood chips in a gasifier stove and found higher efficiency when pellets were used because of their higher bulk density.

The Mimi Moto cookstove, designed by a Netherlands-based company, is a forced-draft gasifier stove fueled by biomass pellets typically made of sawdust from local lumber mills. It has been implemented as a cleaner alternative to cooking in 25 countries in Asia and Africa (Mimi Moto, 2021) and is one of two biomass cookstoves to achieve Tier 4 (best) status for indoor emissions, efficiency, and overall emissions based on the 2012 Water Boiling Test (WBT) standards (Colorado State University, 2015). A new tiering system was published alongside the new International Organization for Standardization (ISO) updated

standard laboratory testing protocol (ISO, 2018a, 2018b) wherein Tier 5 is the cleanest level and Tier 0 represents traditional (i.e., unimproved) solid fuel stoves. Within this ISO tier framework, Champion et al. (2021) found the Mimi Moto CO and  $PM_{2.5}$  emissions in Tiers 5 and 4, respectively, further highlighting the low-emitting performance of this solid fuel stove.

However, emissions from semi-gasifier stoves have been shown to be highly variable and sensitive to stove design, fuel type, fuel moisture content, secondary air velocity/inlet geometry, and operation mode (Carter et al., 2014; Jetter et al., 2012; Kirch, Birzer, et al., 2016; Tryner et al., 2016, 2014; Varunkumar et al., 2011). Champion and Grieshop (2019) reported that PM<sub>2.5</sub> emission factors from the dirtiest Mimi Moto field tests (90th percentile) overlapped with the cleanest wood (10th percentile) and charcoal (60th percentile) stove tests, likely due to variations in stove operation. Increased CO and PM<sub>2.5</sub> emission rates have been observed when stoves transition from gasifying pellets to burning leftover char (Kirch, Birzer, et al., 2016; Kirch, Medwell, and Birzer, 2016; Mukunda et al., 2010; Tryner et al., 2016, 2014; Varunkumar et al., 2011) and when new pellets are added on top of a hot char bed, a practice observed during field studies (Lobscheid et al., 2012; Maddalena et al., 2014; Tryner et al., 2016, 2014). Tryner et al. (2016) found CO emissions using default stove design parameters 36 % and 81 % lower than emissions during refueling and burnout, while Maddalena et al. (2014) found "typical burn, no refuel" PM<sub>2.5</sub> emissions 20 % lower than those with refueling. Additionally, startup material has been shown to play a considerable role in total cookstove CO and PM<sub>2.5</sub> emissions, but to our knowledge has yet to be explored for a gasifier stove with a batch, top down burning configuration (Fedak et al., 2018).

Relatively little is known about particle number emissions of forceddraft gasifier stoves, but it has typically been found that they typically emit more UFPs per mass of fuel, energy delivered, and time than traditional cookstoves (Bilsback et al., 2019; Jathar et al., 2020; Just et al., 2013; Shen et al., 2017). Previous studies report gasifier particle number size distribution mode diameters ranging from below 10 nm to 24 nm, but whether the distribution is uni- or bi-modal is dependent on operation condition (Caubel et al., 2018; Jathar et al., 2020; Just et al., 2013; Shen et al., 2017). Similar to other pollutants, particle number emissions are sensitive to secondary air flow rate and velocity (Caubel et al., 2020; Caubel et al., 2018). While studies have investigated varied operation of other gasifier cookstoves, the impacts of startup material, burning leftover char, and refueling have not been explicitly explored in the context of the widely distributed Mimi Moto stove. Therefore, there is a need for a systematic exploration of how operational details may influence in-use emissions, for both this stove and for other/future gasifier stove designs.

To address the gaps identified above, our study explores how different operation conditions observed in the field lead to increased emissions not typically reflected in lab studies. Specific objectives of our study are to:

- measure emission rates of Startup, Shutdown, and Refueling operation conditions with the Mimi Moto forced-draft gasifier stove and compare these to field results from Champion and Grieshop (2019),
- 2) characterize emission rates for operation phases and describe realtime emissions performance for each operation condition,
- quantify particle number emission factors and size distributions for operation under different conditions,
- provide guidance to the stove manufacturer, distributors, and research community on operation practices associated with lowest pollutant emissions.

#### Methods

Stove and testing protocols

The Mimi Moto cookstove utilizes an internal fan to force air from the bottom upward into two concentric chambers, driving primary air into the internal chamber and secondary air between the internal chamber and external walls. Mimi Moto provides internal chambers of three sizes to meet varied cooking needs. For this study, only the medium sized chamber was used (height = 186 mm, diameter = 85 mm) as it is a representative average of the three chambers and widely used in homes. Table S1 and Fig. S1 show dimensions and pictures of the three chambers. We burned domestically-sourced hardwood pellets shown in Fig. S2. Pellets are made of 100 % hardwood; no additional materials are used as binder. However, use of different materials to make pellets, such as straw, sawdust, peanut hulls, or crop residue, may have large influences on emissions (Champion et al., 2020; Puzzolo et al., 2019).

We conducted tests over two years with their respective standard protocols: the WBT in 2018 and the ISO 19867-1 in 2020. The WBT is a laboratory-based testing protocol developed to measure emissions and stove efficiency from heating water in a cooking pot (Clean Cooking Alliance, 2014), last updated in 2014. The WBT consists of three phases: high-power cold-start, high-power hot-start, and a 45-minute low-power simmer. Only the cold start and simmer phases were conducted in this study since hot start is targeted towards stoves with high thermal mass, unlike the Mimi Moto (Clean Cooking Alliance, 2014).

In 2018, the International Organization for Standardization introduced ISO 19867-1, an updated laboratory testing protocol for emissions, performance, safety, and durability of cookstoves (hereafter the ISO), replacing the WBT as the standard for laboratory emissions testing protocols (ISO, 2018a). The goal of the new ISO protocol was to improve versatility, quality assurance, and adoptability across different testing facilities. The ISO protocol includes three phases (high, medium, and low power; hereafter ISO-High, ISO-Med, and ISO-Low), is ignited with kerosene, and is conducted with separate PM filter sets per phase. Each phase lasts for approximately 30 min with an end time determined by either the water temperature dropping 5 °C from maximum temperature observed during the burning phase or 5 min after the ~30-minute burn. The ISO phases are designed to measure emissions over the full power range of the stove; however, for this study, the protocol was modified to use the same sized stove chamber (medium) for each power level for a more direct comparison between operation conditions. By considering the energy release rate from combustion (firepower) rather than cooking task as in the WBT, the ISO protocol could be more generalizable and representative of field use with less bias on stove design. However, it is also more complicated and requires trial test sequences. It also, like the WBT protocol, includes ambiguities that allow for discrepancies between testing facilities and operators. Champion et al. (2021) compared WBT and ISO protocols and found similar tier ratings for Mimi Moto emissions.

#### Testing matrix

Modified operating conditions were selected to mimic common procedures observed during field measurements and were categorized as Startup, Shutdown, or Refueling approaches, detailed in Table 1. Table S2 details specific procedures for each test type, including ignition methods, fuel masses, and durations. We categorize tests on a threelevel hierarchy based on approach, mode, and phase. 'Approach' refers to the overall test condition and the metric being varied (Startup, Shutdown, or Refuel). 'Mode' refers to the specific test type within an approach (e.g., Startup-Kero, Shutdown-Min). 'Phase' refers to the divisions within a mode (e.g., burn or burnout phase of Shutdown-Min). The two Startup modes varied how the pellets were ignited, either with kerosene or kindling. The Shutdown modes had two phases: a 30-minute "burn" at either minimum or medium fan speed to mimic ISO and a 45-minute "burnout" with fan off, or at minimum, medium, or maximum speeds to mimic the simmer phase of WBT (Mimi Moto fan speed dial shown in Fig. S3a). The Refuel modes were characterized by the height of charred pellets added for re-ignition atop a baseline mass of new pellets within the chamber. The low height was 1 cm above baseline (directly below secondary air holes) and the high height was 4 cm above baseline (top of chamber). We chose these heights as the high height was sometimes observed in the field despite instruction to only fill to the low height. Fig. S3b shows a diagram of Refuel mode charred pellet heights. The charred pellets were created by first burning pellets at maximum fan speed until the flame visually died out (42  $\pm$ 4 min after test start). The char was then added at the specified height atop new pellets and burned at maximum fan speed until the flame visually stabilized (19  $\pm$  5 min after refuel start). All modes except Startup-Kero and Startup-Kind were ignited with 30 g of kerosenesoaked pellets. Startup-Kero was ignited by drizzling 10 mL of kerosene atop dry pellets and Startup-Kind was ignited with a 1 cm thick layer of wood chips and sawdust.

Testing was completed in two batches, during fall 2018 and spring 2020. The tests completed in 2018 followed the WBT, which consists only of Startup approaches, while the tests completed in 2020 followed the ISO after its publication. While ISO calls for five replicates, due to the

**Table 1**Operation conditions and testing protocol by approach.

Approach	Protocol (Year)	Varied metric	Mode	Phase	Mode metric	Replicates
Baseline	Modified ISO (2020)	n/a	Baseline	High Power Med Power Low Power	n/a	3
Startup (SU)	WBT (2018)	ignition fuel	SU-Kero	Burn <sup>a</sup> Burnout	Kerosene	7 <sup>b</sup>
			SU-Kind	Burn <sup>a</sup> Burnout	Kindling	6
Shutdown (SD)	Modified ISO (2020)	fan speed	SD-Off	Burn Burnout	Min (1°) Off	3
			SD-Min	Burn Burnout	Min (1 <sup>c</sup> ) Min (1 <sup>c</sup> )	3
			SD-Med	Burn Burnout	Med (3 <sup>c</sup> ) Med (3 <sup>c</sup> )	3
			SD-Max	Burn Burnout	Min (1°) Max	3
Refuel (RF)	Char Production and Refuel (2020)	char height	RF-Low	Char Prod. Refuel	Low (1 cm)	3
			RF-High	Char Prod. Refuel	High (4 cm)	3

<sup>&</sup>lt;sup>a</sup> Startup phases are not investigated separately as only the influence of startup method is of interest for this approach.

b Only 6 PM<sub>2.5</sub> filters.

<sup>&</sup>lt;sup>c</sup> Fan speeds correspond to the first edition fan from Mimi Moto.

large test matrix and consistency between replicates, we only conducted three replicates for the 2020 batch of testing. A higher number of replicates for the 2018 batch were conducted because the less defined testing procedure led to more variability between replicates. Additional simplified variations were completed during pilot testing for Shutdown and Refuel approaches (Fig. S4a-b).

#### Measurement methods

Laboratory testing was conducted under a total capture hood (described in detail in Reece et al., 2017). Emissions were sampled through a duct at 415 to 630 m $^3$  h $^{-1}$  and a slipstream was sampled coaxially from the duct via a 9.5 mm OD copper tubing and routed to instruments. Flow rate in the duct was measured using a Nailor 36FMS flow grid by averaging the pressure drop in the four quadrants of the duct measured by a Dwyer MS-121-LCD pressure transmitter. Duct temperature was measured with a LabJack EI1034 temperature probe and water temperature in the pot and stove flame temperature were measured using Type K thermocouples.

We sampled emissions using the STove Emissions Measurement System (STEMS), a portable instrument package designed for indoor cookstove emissions measurement. The original version (STEMS-1) and an updated model (STEMS-2) were used for fall 2018 and spring 2020 tests, respectively, and are described in detail elsewhere (Islam et al., 2020; Wathore et al., 2017). Both systems collected real-time measurements of CO<sub>2</sub>, CO, particle light scattering at 635 nm wavelength, temperature, and relative humidity. An AE-51 MicroAeth is also integrated to measure real-time particle light absorption (BC) at 800 nm wavelength. Two parallel 47 mm filter trains containing a bare quartz fiber filter and a quartz filter behind a Teflon filter were used for gravimetric (Teflon) and thermo-optical organic and elemental carbon (quartz) analysis (Wathore et al., 2017). Two handling and one dynamic blank filter sets were collected throughout the 2020 testing process to adjust for any filter handling errors and had an average increase in mass within microbalance tolerance comparable to previous deployments of the STEMS (Champion & Grieshop, 2019; Islam et al., 2020). Teflon filters were weighed before and after testing inside an environmentally controlled microbalance and quartz filters were analyzed in a Sunset Laboratory Carbon Aerosol Analyzer (see Wathore et al., 2017 for additional information on filter analysis). The 2020 batch of testing also collected particle number emissions and size distribution measurements using a TSI Scanning Mobility Particle Sizer (SMPS) for particle diameters ranging from 15 to 685 nm with a scan time of 140 s. Although the SMPS collected particle number count for particles of diameter up to 685 nm, particles >100 nm accounted for <1 % of total particle number, and thus particle number data presented here can be considered to represent UFPs. At least 10 min of background concentrations were measured with both the STEMS and SMPS before stove ignition for background correction of all pollutants. A background particle mass concentration from the SMPS background particle number concentration (2.0 cm $^{-3}$ ) was calculated as 0.021 µg m $^{-3}$  (assuming  $1.0 \mathrm{~g~cm}^{-3}$  particle density).

# Data analyses

#### Emission rate and factor calculations

Pollutant emission rates (ERs) and fuel-based emission factors (EF $_{\rm m}s$ ) were calculated using the total capture method as described in ISO 19867-1. For ERs, pollutant concentrations were averaged over the period of interest (e.g., entire test, test phase) and multiplied by the test average duct flow. For the last six tests completed, the duct flow inadvertently exceeded the range of manometer used with the flow grid, likely due to external changes in the lab ventilation system. To estimate the correct flow, the carbon balance method was used, which assumes all fuel carbon is emitted as CO or CO $_2$ . Carbon is also present in emitted hydrocarbons, methane, and PM, but at negligible

concentrations. While we did not measure hydrocarbons or methane in this study, a lab study with the Mimi Moto found that 0.036 % and 0.0% of carbon was released as hydrocarbons and methane, respectively (Champion et al., 2020). In our study, 0.025 % of carbon was released as PM on average. The carbon emitted can be converted to dry fuel consumed using a mass-weighted carbon content including both wood and kerosene mass, assuming 0.5 kg C per kg dry wood and 0.85 kg C per kg kerosene (Roden et al., 2006; Smith et al., 1993). A fuel moisture content of 8.6 % was used to correct to dry wood mass in pellets (Champion & Grieshop, 2019). This value was chosen from analysis completed by Champion and Grieshop (2019). Additional fuel moisture analysis two years after testing found mildly lower fuel moisture (6.1%). The average value of 8.6 % was used as it is more representative of recently-produced pellets; note that emission factor calculations have relatively little sensitivity to this small variation in moisture values. Using the average carbon concentration determined from the carbon balance and the dry fuel consumption rate, the duct flow was estimated for the six tests (e.g., the six tests with manometer readings exceeding instrument range). An average of corrected flows was used in further calculations for these tests. Additional details are described in SI

Additionally, the carbon balance method was used as a quality check by comparing g C kg fuel $^{-1}$  calculated with both carbon balance and total capture methods (ISO, 2018a; Roden et al., 2006; Wathore et al., 2017). Excluding the six tests mentioned above that exceeded the duct flow meter manometer range, the average percent difference between the carbon balance and total capture calculated carbon  $\rm EF_{m}s$  for all tests including pilot tests was 31 %. To help correct this high bias, we completed a post-testing duct flow calibration. When the updated duct flow calibration was applied to the total capture carbon  $\rm EF_{m}$  calculations, the average percent difference between the total capture and carbon balance  $\rm EF_{m}s$  decreased from 31 % to 1.0 %. This decrease suggests the source of systematic discrepancy between the two methods was correctly identified as a miscalibrated duct flow meter. More details on this procedure are included in SI Section S2.

 $EF_ms$  were calculated by multiplying the background-corrected average pollutant concentration by average duct flow and test duration and dividing by the dry mass of fuel consumed. This fuel-based emission factor was converted to an energy delivered-based emission factor ( $EF_d$ ) by dividing by the fuel lower heating value (17.3 MJ kg $^{-1}$ ; Grieshop et al., 2011) and calculated cooking thermal efficiency accounting for char (61  $\pm$  5 %), as described in ISO 19867-1. Due to the availability of necessary measurements, we could only calculate thermal efficiency on a per test basis and not per phase. We calculated phase-specific  $EF_ds$  by assuming constant thermal efficiency across phases for each test and using the carbon balance method to estimate phase-specific fuel use. To calculate time-resolved number  $EF_m$  distributions, we converted per-scan number concentrations measured by the SMPS using the carbon balance method.

ERs and EFs were then compared within the ISO TR 19867-3 tier framework. While ISO tiers are intended for full-range ISO lab results only, they are applied here with modified operation modes for context and as a reference point. These tiers are defined in terms of energy delivered emission factors but can be equated to emission rates as described in ISO TR 19867-3.

#### Cumulative instantaneous CO emissions

We created a cumulative distribution of CO mass emissions to analyze the instantaneous changes in emissions throughout a test. The 1 Hz CO concentrations were averaged to 1-minute resolution and corrected for background concentration. From test ignition to test end, using an approach similar to Preble et al. (2014) however not normalizing with respect to total mass emitted, a cumulative distribution was computed by adding each 1-minute averaged mass of CO emitted to the mass of the preceding time interval:  $M_{CO,\ t} = M_{CO,\ t-1} + \Delta CO_{\Delta t} Q\Delta t$ , where  $M_{CO,\ t}$  is the cumulative mass of CO emitted (mg)

until time t,  $M_{CO,\ t-1}$  is the cumulative mass of CO emitted (mg) from the previous time,  $\Delta t$  is the time interval (here 1 min),  $\Delta CO_{\Delta t}$  is the increase in CO concentration above background levels (mg m<sup>-3</sup>) for that time interval, and Q is the flowrate through the duct.

#### Startup to steady state ER ratio

We developed CO startup to steady state ER ratios to compare ignition methods across approaches. Steady state was defined as the period where  $CO_2$  was approximately constant, determined by taking the difference between each  $CO_2$  reading and performing a rolling average for the previous 10 differences. If the 10-second average difference between  $CO_2$  readings was <10 ppm, the period was considered at steady state. The  $CO_2$  over this period was averaged, and the startup period was defined as the test ignition time to the time it took to reach 90 % of the average steady state  $CO_2$ .

#### Limit of detection

Limits of detection (LODs) for PM<sub>2.5</sub>, OC, and EC were calculated following an approach described elsewhere (Armbruster & Pry, 2008; Islam et al., 2020; Weyant et al., 2019) and are detailed in SI Section S3. Based on these criteria, 32 %, 53 %, and 47 % of PM<sub>2.5</sub> mass, OC, and EC measurements, respectively, for all tests and pilot tests were below their LOD. While this is not ideal, this is a relatively clean stove in terms of particulate emissions and these percentages are within reasonable range for a university facility. For reference, Champion et al. (2021) conducted ISO tests for the Mimi Moto at a 'reference' facility (US EPA's Household Energy Laboratory in Research Triangle Park, NC, USA) and had 0.0 %, 21 %, and 8.0 % of PM<sub>2.5</sub>, OC, and EC measurements below their LOD.

Baseline PM<sub>2.5</sub> ER averages including (2.5  $\pm$  1.2 mg min<sup>-1</sup>) and excluding (2.8  $\pm$  1.0 mg min<sup>-1</sup>) below-LOD filters were not significantly different (via Wilcoxon ranksum test based on non-normal distributions). Baseline OC and EC ER averages with (0.43  $\pm$  1.0, 0.13  $\pm$  $0.12~\mathrm{mg~min^{-1}})$  and without  $(1.2\pm1.4,\,0.34~\mathrm{mg~min^{-1}})$  LOD filters included were also not significantly different. For group-wise analysis, replicate tests with emission metrics below the LOD were adjusted to the LOD value and metrics below zero were adjusted to zero for inclusion in reported average calculations (Champion et al., 2021). It should be emphasized here that the motivation of this study was to better understand drivers for high-emission events (e.g., 90th percentile of Champion & Grieshop, 2019 field emissions), not necessarily to characterize low-emitting conditions. Therefore, emission factors reported here should be considered upper bounds, and the Mimi Moto emissions reported in Champion et al. (2021) likely provide a better basis for ISO protocol comparison.

#### Results

## Test emission rates

Fig. 1a-b shows emission rates for CO and  $PM_{2.5}$  for the modified ISO Baseline and each operation condition divided by approach. Champion and Grieshop (2019) CO and  $PM_{2.5}$  field test ERs are included for comparison. ISO performance tiers are denoted in Figs. 1 and 2 by green shading to provide reference between emissions of our modified operation tests and the levels for full-range ISO lab results. Figs. S5–13 show time series of  $CO_2$ , CO, and particle number (excluding Startup-Kero and Startup-Kind) concentrations of one test replicate for each mode.

Lab values are generally low, with CO and PM<sub>2.5</sub> ERs ranging from 5.7 to 190 and from 0.0 (non-detect) to 8.0 mg min<sup>-1</sup>, respectively. Median ERs of CO (25 mg min<sup>-1</sup>) and PM<sub>2.5</sub> (1.4 mg min<sup>-1</sup>) are below the 10th and 20th percentiles of respective field ERs. However, Refuel-High ERs overlap with field emissions, consistent with observations from Champion and Grieshop (2019), who found that half of their high-emitting tests included refueling. Refuel-High average CO

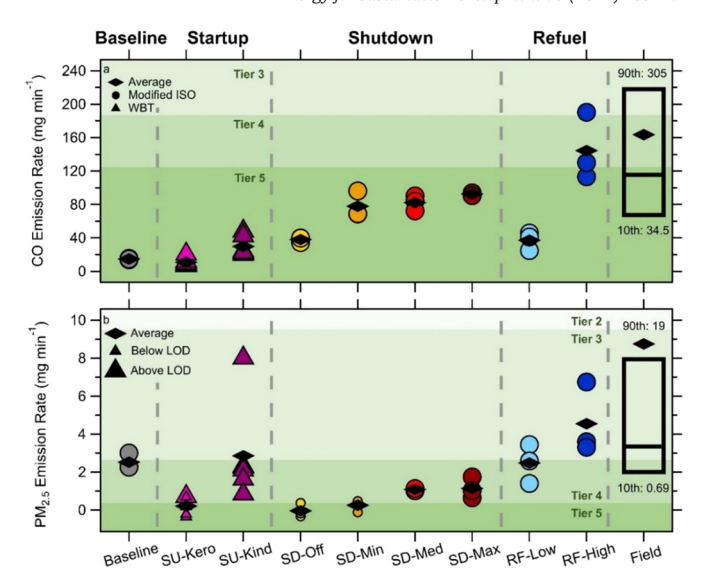


**Fig. 1.** (a) CO and (b) PM<sub>2.5</sub> emission rates for each operation mode. Shutdown labels represent fan speed during burnout phase of test and Refuel labels represent pellet refuel fill height. The 'Field' boxplot shows data from Champion and Grieshop (2019). WBT modes are represented by triangles while modified ISO is represented by circles. PM<sub>2.5</sub> emission rate data points represented by smaller circles are tests with filter weight measurements below the limit of detection. Green shading denotes ISO performance tiers for context but are not indicative of full-range ISO Mimi Moto emissions tiers.

 $(PM_{2.5})$  ER was 140 (4.5) mg min<sup>-1</sup> while field average CO  $(PM_{2.5})$  ER was 160 (8.7) mg min<sup>-1</sup>. Baseline test emissions were consistent with Tier 5 for CO and Tier 4 for  $PM_{2.5}$ , both in terms of ER and  $EF_d$  (Fig. S14). Modified operation tests generally emit consistently with Tier 5 for CO ER and Tier 4 for  $PM_{2.5}$  ER, with a few exceptions: Refuel-High CO ERs in Tier 4, Startup-Kind and Refuel-High  $PM_{2.5}$  ERs in Tier 3, and Shutdown-Off  $PM_{2.5}$  in Tier 5 (however the latter results were below LOD).

# Modified ISO and WBT baseline comparison

The two left-most sets of data points in Fig. 1 show a comparison of CO and PM<sub>2.5</sub> emission rates measured during ISO and WBT baseline testing, indicating general consistency across protocols, with some minor but statistically significant differences. Mean CO ER was similar for ISO and Startup-Kero (WBT baseline), 15 vs 11 mg min $^{-1}$ . Mean PM<sub>2.5</sub> ER was 80 % lower for WBT vs ISO tests, with 95 % confidence intervals on the means of 0.19–0.84 and 1.9–3.2 mg min $^{-1}$ , respectively.

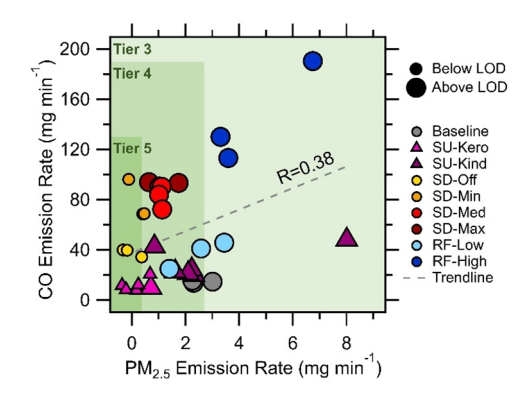


**Fig. 2.** CO versus  $PM_{2.5}$  emission rates for all operation modes with mapped equivalent ISO tiers. Triangles are tests using WBT protocol, circles used modified ISO, and smaller symbols denote  $PM_{2.5}$  filters below LOD. Green shading denotes ISO performance tiers for context.

The Wilcoxon ranksum test suggests that the ISO  $PM_{2.5}$  ER average is significantly higher than that for WBT tests, likely because the longer, lower-power simmer phase in WBT pulls down the test average  $PM_{2.5}$  emission rates. Most  $PM_{2.5}$  was emitted during startup with little contribution during the simmer phase (reinforced in Fig. 4c); therefore, WBT tests' longer periods of lower  $PM_{2.5}$  emissions reduces the overall  $PM_{2.5}$  emission rate averages.

#### Varied operation mode emission rates

Fig. 1 also summarizes CO and PM<sub>2.5</sub> emission rates across the modified operation approaches. As expected, Startup approach has a substantial effect on test emissions. Kindling ignition emitted 2.7 and 5.6 times more CO and PM<sub>2.5</sub> than kerosene, respectively, with Startup-Kero within PM<sub>2.5</sub> Tier 4 and Startup-Kind averaging slightly greater than the PM<sub>2.5</sub> Tier 4 cutoff, placing it in Tier 3. Additionally, Startup modes were more variable than other modified operation modes, likely due to a less defined protocol. For example, the highest Startup-Kind PM<sub>2.5</sub> ER (Fig. 1b) corresponds to a test where the kindling ignition event was almost three times longer than other tests, suggesting a less effective ignition due to kindling properties or technique. Higher PM<sub>2.5</sub> ERs for Startup-Kind compared to Startup-Kero are likely attributable to an inefficient ignition not sustaining high enough temperatures in the combustion chamber to oxidize PM.

Fan speed during shutdown had a substantial impact on CO, but less on PM<sub>2.5</sub>, consistent with the solid-phase oxidation form of combustion seen in charcoal stove emissions, in which lower combustion zone temperatures inhibit oxidation of CO (Bilsback et al., 2019, 2018; Eilenberg et al., 2018; Jetter et al., 2012). CO ERs increased with higher fan speeds during the burnout phase, increasing 105 % from Shutdown-Off to Shutdown-Low, 5.5 % from Shutdown-Low to Shutdown-Med, and 13 % from Shutdown-Med to Shutdown-High. PM<sub>2.5</sub> shutdown ERs show a similar but less obvious trend than CO. Shutdown-Off and Shutdown-Min modes average lower ERs, 0.16 and 0.35 mg min<sup>-1</sup> respectively, than Shutdown-Med and Shutdown-Max modes, both at 1.1 mg min<sup>-1</sup>. By increasing the fan speed during burnout, we increase the amount of cool air entering the chamber, likely decreasing combustion temperature. This cooling inhibits oxidation of particulate matter and CO to CO<sub>2</sub>. This hypothesis is reinforced by the increasing CO ER trend with increasing fan speed; an abrupt increase from Shutdown-Off to Shutdown-Min, then smaller increases thereafter. This abrupt increase suggests that turning the fan on to any level cools the combustion zone enough to slow oxidation.

Refueling approach had the largest impact on both CO and PM<sub>2.5</sub> emission rates, with Refuel-High emitting 3.9 and 1.8 times more CO and PM25 than Refuel-Low; Refuel-High also emitted 9.8 and 1.8 times more CO and PM<sub>2.5</sub> than Baseline. Refuel-Low emitted 2.5 times more CO than Baseline but PM<sub>2.5</sub> within 3.0 % of Baseline PM<sub>2.5</sub>. Similar to Startup tests, the less defined protocol for the Refueling approach led to greater variability; the highest Refuel-High PM<sub>2.5</sub> ER (Fig. 1b) corresponds to a test that was 15 min longer than the other two tests, likely because the flame took longer to visually stabilize in the refuel phase. The high CO and PM<sub>2.5</sub> ERs from Refuel-High tests are likely due to the blocking of the secondary air holes, as defined by the protocol, limiting air-fuel mixing and leading to less complete combustion (Turns, 2012). Refuel-High had the largest CO and second largest PM<sub>2.5</sub> ER of the tested operation modes and had the largest difference in emissions observed across all approach categories. Thus, emission rates are more sensitive to refuel height than burnout fan speed or startup method. Higher Startup-Kind and Refuel PM<sub>2.5</sub> ERs are consistent with Champion and Grieshop (2019); of their PM<sub>2.5</sub>  $EF_ms \ge 90$ th percentile, half the tests used kindling for ignition and half the tests included refueling.

As expected, particle number emission rates (shown in Fig. S15) closely resemble the trends seen in Fig. 1b for PM<sub>2.5</sub> ERs for Baseline, Shutdown, and Refuel modes. Baseline particle number ERs fall in the middle of our lab ER range. Shutdown modes have the lowest particle

number ERs, with a slight distinction between lower (Shutdown-Off, Shutdown-Min) and higher (Shutdown-Med, Shutdown-High) fan speeds. Refuel-High has the greatest particle number ERs,  $23\,\%$  higher than Refuel-Low.

Fig. 2 plots CO versus PM<sub>2.5</sub> emission rates for Baseline and all operation conditions along with ISO emission tiers. A direct comparison of CO versus PM<sub>2.5</sub> ER with EF<sub>d</sub> Tiers is shown in Fig. S14. Generally, CO and  $PM_{2.5}$  are not monotonically related (R = 0.38), and CO ERs are more variable than PM<sub>2.5</sub> ERs. The lowest emitting condition was Startup-Kero. Baseline was lower in CO and higher in PM ERs than Shutdown modes, which is expected considering the stove operations emphasized in each. Shutdown modes are essentially Baseline tests followed by a 45-minute burnout period. This burnout phase contributes high CO and low PM emissions (Fig. 4), that when included in the overall test-averaged emissions, results in higher CO and lower PM<sub>2.5</sub> ERs than Baseline. For the Shutdown approaches, Shutdown-Off is the lowest emitting while Shutdown-Min, Shutdown-Med, and Shutdown-Max fall into similar CO and PM<sub>2.5</sub> ER ranges. Fig. S16a shows similar trends when comparing CO to particle number emission rates; Shutdown-Off is lowest emitting and other Shutdown modes are similar. PM<sub>2.5</sub> and particle number emission rates are strongly correlated, with a correlation coefficient of 0.92 (Fig. S16b).

#### Elemental and organic carbon emission rates

Fig. 3a-b shows emission rates for EC and OC for Baseline, all modified operation approaches, and Champion and Grieshop (2019). EC and organic matter (OM) make up on average 76 % of  $PM_{2.5}$  mass emitted (n = 8, excludes tests with EC, OC, or  $PM_{2.5}$  masses below LOD). SI Section S4 and Table S3 include calculations and percentages for all tests. Generally, lab values are low and similar across operation modes, ranging from 0.0 (non-detect) to 0.34 mg min<sup>-1</sup> for EC and 0.0 (non-detect) to 3.4 mg min<sup>-1</sup> for OC. Median lab EC (0.15 mg min<sup>-1</sup>) and OC (0.48 mg min<sup>-1</sup>) ERs are equivalent to 20th and 30th percentiles for respective field ERs. While lab EC emissions are relatively consistent across modes, OC emissions show more variability, particularly for Startup approaches. This variability is also evident in Startup  $PM_{2.5}$  ERs (Fig. 1b). Additionally, OC ER averages for Startup-Kind and Refuel modes are 1.9 and 1.3 times higher than other lab modes; therefore, these modes have the highest OC ERs. Low combustion temperatures

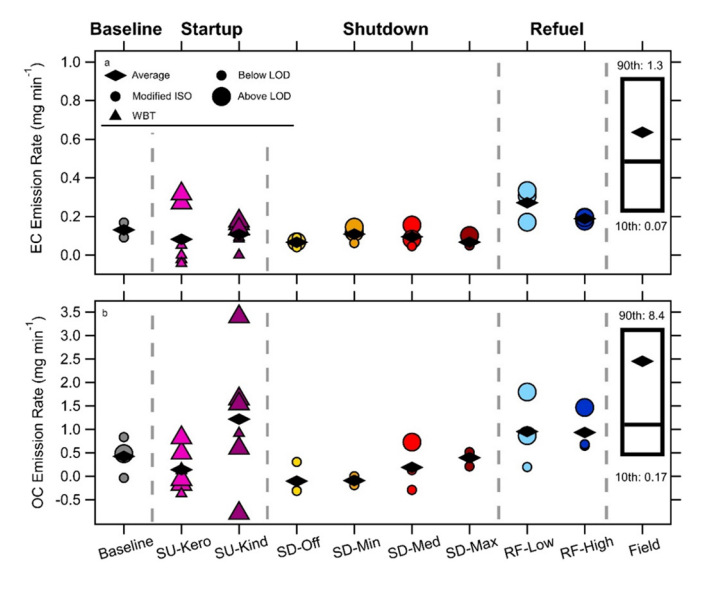


**Fig. 3.** (a) EC and (b) OC emission rates for each operation condition. Shutdown labels represent fan speed during burnout phase of test and Refuel labels represent pellet refuel fill height. The 'Field' boxplot is based on data from Champion and Grieshop (2019). Data points represented by smaller circles are tests that had measurements below the limit of detection.

promote OC formation and are likely in Startup-Kind during ignition, which may possibly explain the highest OC ER observed in this mode.

#### Phase-specific emission rates

To evaluate emissions contributions over test durations for Shutdown and Refuel operation modes, we calculated phase-specific emission rates for the two phases in each mode: burn and burnout phases for Shutdown and char production and refuel phases for Refuel. However, in application, cooking activity likely exceeds the 30-minute burn and 19-minute refuel phases which occurred here, so phase times and their emissions contribution could be weighted differently during real-world use. Fig. 4a-d shows phase-specific CO and particle number ERs for both approaches. Because particle number emissions were time resolved values, we can disaggregate them unlike testintegrated PM<sub>2.5</sub> measurements. Particle number emission rates here include particles ranging from 15 nm to 685 nm but consist 99 % of UFPs. Burn phases for the different Shutdown modes were conducted at either minimum (for shutdown with fan at off, low, and max settings) or medium (for shutdown with fan at medium setting) fan speeds (refer to Table 1). Both Refuel approaches were preceded by the same char production phase, which are thus grouped together in Fig. 4b and d.

For Shutdown modes, CO emission rates were substantially higher during the burnout phase, while particle number emissions were higher during the burn phase. Burn phase CO ERs were similar between fan speeds while burnout phase CO ERs increase with increasing fan speed and were two orders of magnitude higher than burn phase ERs. In contrast, particle number ERs were substantially lower for burnout phase than burn phase (Shutdown-Off and Shutdown-Max were 1 % and 27 % of burn ERs), though they do show the same increasing trend with fan speed. CO ERs were on average 31 times higher in the burnout phase than burn phase, while particle number ERs were 7.9 times higher in the burn phase. When mapping burnout phase CO ERs to ISO tiers, Shutdown-Off remains in Tier 5, but Shutdown-Min, Shutdown-Med, and Shutdown-Max fall to Tier 4.

In contrast, for Refuel modes, both CO and PM $_{2.5}$  emission rates were higher for the refuel versus char production phases. Refuel-Low and Refuel-High refuel phase CO ERs were ~5 and ~24 times higher than char production phase CO ERs, respectively. Refuel-Low and Refuel-High refuel phase particle number ERs were 27 % and 42 % greater than char production phase ERs. The increase in refuel phase ERs from

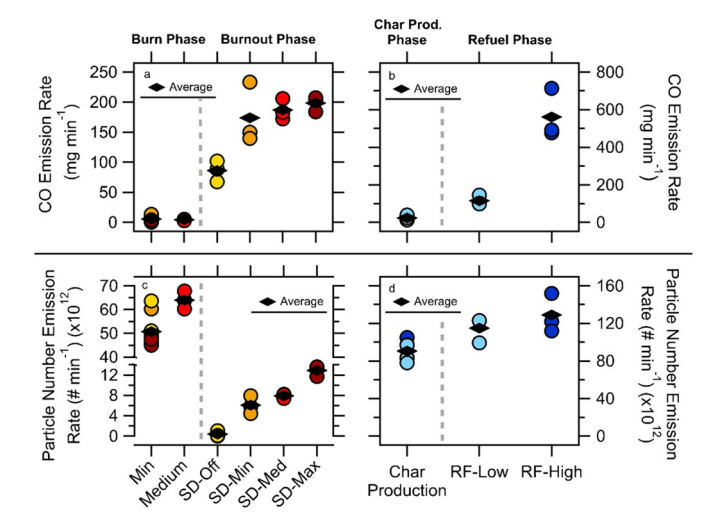


**Fig. 4.** Emission rates of CO for (a) Shutdown and (b) Refuel approaches and particle number for (c) Shutdown and (d) Refuel approaches. Note particle number emission rates include particles ranging from 15 nm to 685 nm per SMPS configurations applied here.

Refuel-Low to Refuel-High is more obvious for CO than particle number; specifically, Refuel-High CO ERs were 4.9 times greater than Refuel-Low, and Refuel-High particle number ERs only 1.1-fold greater. Therefore, the increase in ER from low to high height was 4.4 times greater for CO than particle number, suggesting CO emissions were more sensitive to refuel height. The difference between refuel and char production ERs was greater for CO than particle number, suggesting the char production phase was a bigger contributor to particle number than CO emissions. When considering ISO tiers for CO refuel phases, Refuel-High falls to Tier 1.

Fig. S17a-b shows CO and particle number emission rates for the three power level phases during Baseline ISO testing and shows that the medium power phase had the highest ERs. Baseline CO ERs (averaging 15 mg min $^{-1}$  across all phases) are most consistent with Shutdown burn phase (5.2 mg min $^{-1}$ ) and Refuel char production phase (24 mg min $^{-1}$ ) ERs, while Baseline particle number ERs (averaging 5.4  $\times$  10 $^{13}$  # min $^{-1}$ ) are most consistent with Shutdown burn phase (5.4  $\times$  10 $^{13}$  # min $^{-1}$ ).

# Energy delivered emission factors by shutdown approach

Here we discuss energy delivered emission factors which enable comparison of useful energy and emissions in order to recommend the most desirable condition for users (e.g., using all energy from the fuel before discarding so as to not lose useful energy). Fig. 5a-b shows phase-specific CO and particle number EF<sub>d</sub>s in terms of useful energy delivered for Shutdown approaches. Fig. 4 shows a clear trend of increasing ERs for increasing fan speed during burnout; however, it does not consider that higher fan speeds will deliver more energy than lower fan speeds. Fig. 5 displays phase-specific EF<sub>d</sub>s, while test-averaged CO and PM<sub>2.5</sub> EF<sub>d</sub>s are shown in Fig. S18a-b and generally follow the trends in Fig. 1a-b: increasing CO emissions with increasing fan speed and a shift up in PM<sub>2.5</sub> emissions from lower to higher fan speeds.

Phase-specific EF<sub>d</sub> trends generally resemble phase-specific ER trends shown in Fig. 4a and c; however, burnout phase CO EF<sub>d</sub>s do not increase with increasing fan speed. Instead, Shutdown-Off (7.4 g MJ<sub>del</sub>) and Shutdown-Med (7.3 g MJ<sub>del</sub>) are the highest and Shutdown-Min (5.9 g MJ<sub>del</sub>) and Shutdown-Max (6.0 g MJ<sub>del</sub>) are lowest. Although Shutdown-Max has the highest emission rates, Shutdown-Min and Shutdown-Max have the lowest emissions when normalized by their provided useful energy. Because Shutdown-Min has lower ERs than Shutdown-Max, it is the optimal burnout speed in terms of CO emissions and energy delivered. However, particle number EF<sub>d</sub>s increase with increasing fan speed at burnout (consistent with Fig. 4c), so there is a tradeoff between CO and particle number emissions to consider.

To consider useful heat, we also examine water temperature. Fig. 6 shows the water temperature for each Shutdown mode during the burnout phase. The water temperature for Shutdown-Off immediately

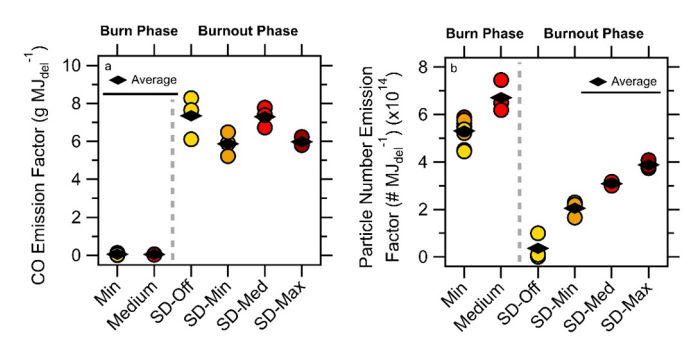


**Fig. 5.** Phase-specifc energy delivered emission factors for (a) CO and (b) particle number for Shutdown approaches. Note particle number emission factors include particles ranging from 15 nm to 685 nm per SMPS configurations applied here.

started decreasing, dropping 13 °C on average in the first 5 min. The temperature decreases for the other modes trend opposite of fan speed, with Shutdown-Min, Shutdown-Med, and Shutdown-Max dropping 7.9, 6.3, and 1.7 °C in the first 5 min. Shutdown-Max remained at average boiling point for the first 15 min, and then had a sudden decrease for the remainder of the burnout phase, finishing with a water temperature lower than all other modes. While Shutdown-Max initially provides the most energy to the water, after 15 min, it loses power faster than for the other modes. Shutdown-Max provides 13 more minutes of boiling than Shutdown-Off but lead to 2.4 and 7.3 times more CO and PM<sub>2.5</sub>. Shutdown-Min resulted in the smallest decrease in water temperature over the burnout period and thus the most energy delivered of the four variations, reinforcing that it is the prefered fan speed if burnout is necessary.

In summary, the most CO and  $PM_{2.5}$  emissions can be mitigated by avoiding burnout or turning the fan off. However, if stove users want or need more heat for a long period of time after flameout, minimum fan speed can provide more heat slowly with the least emissions. If users want boiling temperature briefly after flameout, maximum fan speed can achieve this, but results in substantially greater emissions.

# Kerosene versus pellet char ignition emissions

Next, we examine how ignition with pellet char, which is the ignition process of the refuel phase for Refuel-Low and Refuel-High, compared to ignition with kerosene. We considered this comparison because reusing pellets is often observed and sometimes encouraged in field settings as the more economic option compared to disposal. To make startup emissions comparable across different operation modes, we normalized startup ERs by their steady state ERs to calculate an ER ratio for Baseline (ISO medium power ignited with kerosene), Refuel-Low, and Refuel-High. Medium power ISO was selected as the kerosene comparison because it was a higher power, hot start, so most similar to the refuel phase of the Refuel approach tests. An ER ratio greater than one indicates that emission rates were higher during startup than steady state operation, with a higher ratio indicating a greater influence from startup.

Fig. 7a-b shows CO and particle number startup ratios, where generally, ratios increase from Baseline to Refuel-Low to Refuel-High, suggesting that kerosene ignitions are cleaner than those using pellet char. CO ratios were above one for all ignition scenarios and ranged up to 98, indicating that CO ERs during startup were substantially larger than during steady state operation. Particle number ratios ranged from 0.04 to 1.7, where only the Baseline ER ratio averaged below one (0.13). Thus, for Baseline tests, particle number emission rates during startup were lower than during steady state. In contrast, Refuel tests both had particle number ratios above one but only slightly at 1.2

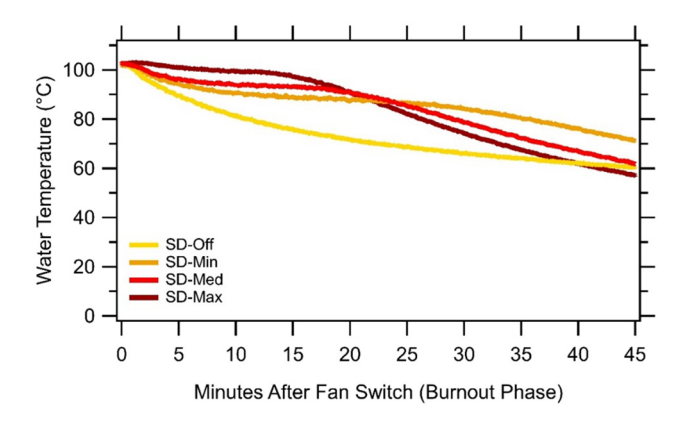
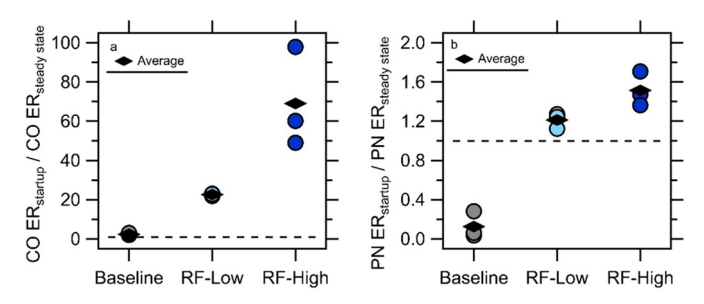


Fig. 6. Water temperature measured in pot during the burnout phase for each Shutdown mode.



**Fig. 7.** Startup to steady state (a) CO and (b) particle number (PN) ER ratios. Black dotted line represents a ratio of one where startup ER and steady state ER are equal.

(Refuel-Low) and 1.5 (Refuel-High). Particle number ratios are two orders of magnitude lower than CO ratios; thus, the increment in CO contribution is much greater than for particle number during startup.

#### Cumulative CO emissions

We now investigate how emissions vary over the entire usage period of the stove by examining cumulative instantaneous emissions. Fig. 8a-d shows the average cumulative distribution of instantaneous CO emissions for Baseline and modified operation approaches. Time series plots of CO<sub>2</sub>, CO, and particle number (excluding Startup-Kero and Startup-Kind) concentrations of one test replicate for each mode are shown in Figs. S5–13. CO emissions for Baseline tests increase somewhat linearly with time with a relatively small increment from startup emissions in the first 3 min, which we also see in Fig. 7a with an average CO startup to steady state ER ratio of 2.4.

Startup-Kero and Startup-Kind CO emissions show similar trends over test duration, with 36 % and 60 % of CO emitted in the first 15 min followed by little to no emission until a spike in the last 10 min due to burnout. However, Startup-Kind emitted 4.1 times as much CO in the first 15 min as Startup-Kero. Startup-Kind emitted more CO in the first 10 min than the entire duration of Startup-Kero tests, demonstrating the major influence startup approach can have on full test emissions. This initial increase in CO for Startup-Kind compared to Startup-Kero reinforces that a kindling ignition could be associated with lower combustion temperatures that inhibit oxidation of PM<sub>2.5</sub> and CO.

For Shutdown modes, cumulative CO emissions were highest for Shutdown-Max and lowest for Shutdown-Off. The burn phase of the Shutdown tests contributed little to total CO emissions (on average  $<5\,\%$ ). Similarly to Baseline emissions, there was a quick increase during the first 5 min due to startup. However, from 5 min to the end of the burn phase, Shutdown CO emissions on average only increased by 42 % while Baseline emissions increased 206 % for the same increment. With the exception of Shutdown-Off, increasing fan speed during burn-out led to an earlier and sharper increase in emissions. Shutdown-Off burnout emissions increased sooner than other modes, but at a much lower rate. Almost all CO emitted during the refuel phase was emitted in the first 5 min, 76 % and 97 % for Refuel-Low and Refuel-High, and then emissions flatten out for the remainder of the test. Refuel-High emits 5.8 times as much CO as Refuel-Low.

We also investigated how carbon emissions vary over the entire usage period of the stove as a proxy for real-time fuel loss. Fig. S19 shows the average cumulative distribution of instantaneous carbon  $(CO+CO_2)$  emissions for Baseline and modified operation approaches. For Baseline, Startup, and Refuel approaches, cumulative carbon emissions were largely linear, signifying constant carbon emission rates (thus fuel consumption rates) over the test durations. For Shutdown approaches, cumulative carbon emissions were linear during the burn phase then flattened during the burnout phase, signifying constant

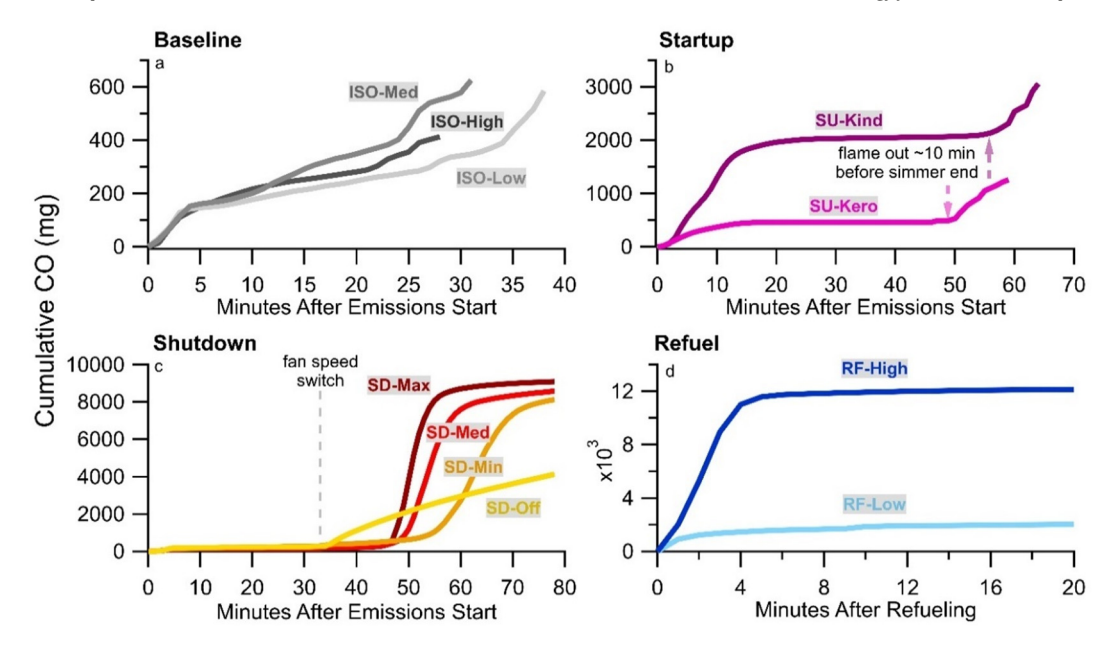


**Fig. 8.** Cumulative CO emissions averaged across replicates for (a) modified ISO Baseline and (b) Startup, (c) Shutdown, and (d) Refuel approaches. For Baseline, Startup, and Shutdown approaches, the mass of CO emitted was added cumulatively after ignition until test completion. For Refuel approach, mass of CO emitted was added cumulatively after char addition. Note the y-axis scales are different across approaches to maximize clarity for comparisons across modes within each approach. For side-by-side average comparisons between approaches, see Figs. 1 and 3.

carbon emissions during burning and then little contribution to the total carbon emitted during the burnout phase.

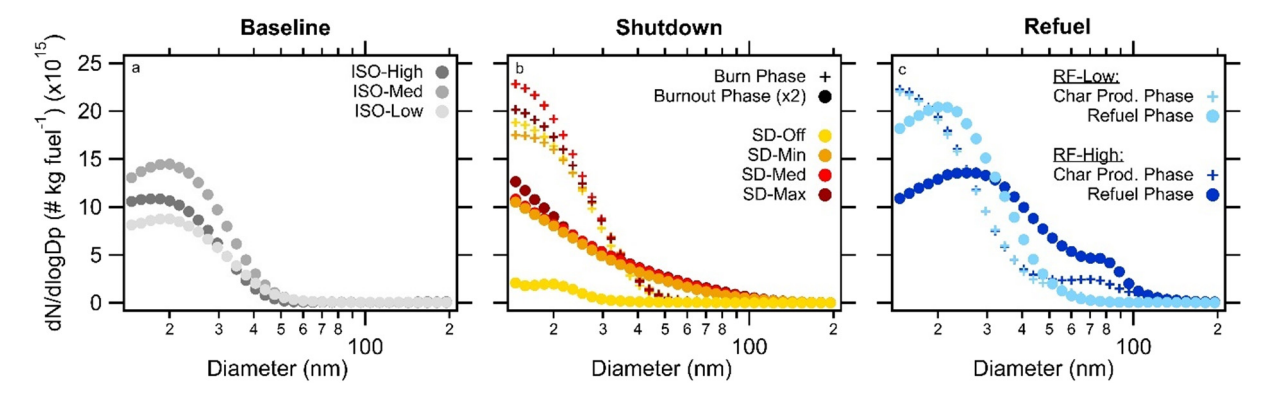
#### Particle number size distributions

Fig. 9a-c shows average particle size distributions for Baseline, Shutdown, and Refuel approaches divided into each conditions' respective phases. The burnout phase distribution in Fig. 9b is multiplied by a factor of 2 for clarity. Generally, almost all particles emitted for all approaches are ultrafine (<100 nm in diameter). In some cases, the mode diameter of distributions fell below our low size cutoff of 15 nm, particularly for Shutdown burnout phases. Mode diameters ranged from below 15 to 75 nm, with primarily unimodal distributions. Mostly UFP emissions, rather than larger particles, from the Mimi Moto are unsurprising as UFPs can form from condensation of organic vapors, typically at lower temperatures. Because gasifier stoves often have both lower temperature regions and less particle surface area to condense onto, nucleation and condensation are likely to occur (Bilsback et al., 2019; Hinds, 2012; Khalek et al., 2000).

For Baseline power phases (Fig. 9a), ISO-Med particle emissions are the highest and ISO-Low the lowest (consistent with Fig. S17b). All ISO phases have a similar mode diameter, approximately 20 nm. Baseline particle emissions fall between Shutdown burn and burnout phase emissions (Fig. 9b) and are similar in magnitude to Refuel-High refuel phase's smaller mode (Fig. 9c).

Both Shutdown burn and burnout phases had similar size distributions across particle diameters for all fan speeds, increasing in particle emissions with increasing speed at burnout. However, it appears that at least half of the particle number fall below our SMPS lower cutoff diameter of 15 nm. The burn phase distributions appear to level off at their mode diameter around 15 nm while the burnout phase distributions appear to have a mode diameter smaller than that captured by the SMPS.

For Refuel modes, the char production average size distribution was consistent between fill heights at diameters below 50 nm, but a second mode appeared in the Refuel-High char production phase distribution, with a mode diameter of 75 nm. Approximately half of the char production phase distributions are captured as the rest of the distribution falls below the cutoff diameter. A second mode also appears in the Refuel-



**Fig. 9.** Average particle size distributions normalized as EF<sub>m</sub>s of (a) Baseline, (b) Shutdown, and (c) Refuel operation modes. Distributions are divided into ISO phases for Baseline, burn and burnout phases for Shutdown modes, and char production and refuel phases for Refuel modes. The burnout phase distributions are multiplied by a factor of two for clarity. Note particle number emission factors include particles ranging from 15 nm to 685 nm per SMPS configurations applied here; however, the x-axis scale was truncated for clarity as 99 % of particles emitted were UFPs.

High refuel phase distribution. From the time series image plot of particle number concentration (one Refuel-Low and Refuel-High replicate shown in Fig. S20a-b), there was an abrupt increase in concentration and mode diameter during Refuel-High transition from char production to refuel phase, appearing as a second mode. This brief second mode was also apparent in Refuel-Low image plots but at lower concentrations and thus did noticeably influence averaged particle size distributions. The smaller mode in Refuel-High refuel phase emissions has a greater mode diameter than those from Refuel-Low. The Refuel-Low refuel phase distribution resembles Baseline distributions (Fig. 7a) but with an EF $_{\rm m}$  that is 1.4 times the highest Baseline test (ISO-Med). Therefore, generally, larger particles were emitted during Refuel-High, but more, smaller particles were emitted during Refuel-Low. Preventing secondary air flow by blocking these air holes with pellet char led to more emissions of larger particles.

#### Comparison with previous results

We conducted laboratory testing that systematically varied stove operation to attempt to replicate and explain high-emission events observed in the field. We used a relatively recently published protocol that few studies have implemented and an individual, widely used pellet gasifier stove that has been included in few lab studies. Therefore, our study is unique and many results are not readily comparable to existing work. With that caveat, it is still beneficial to place our results in a broader context. Here we compare our results to those from other lab studies examining similar metrics and gasifier stoves.

Few studies have conducted laboratory testing under the updated 2018 ISO protocol due to its recent publication (ISO, 2018a). Our average ISO-High ERs for CO (9.1 mg  $min^{-1}$ ) and  $PM_{2.5}$  (1.8 mg  $min^{-1}$ ) were 97 % and 60 % lower than that reported by Champion et al. (2020), who used the Mimi Moto, hardwood pellets, and ISO protocol. However, average OC (1.6 mg min<sup>-1</sup>) and EC ER (0.24 mg min<sup>-1</sup>) were 13 and 1.7 times higher than Champion et al. (2020). The large discrepancy between CO ERs is likely due to differences in shutdown from "high-phase" definitions. When comparing our baseline ISO and WBT (Startup-Kero) to Champion et al. (2021), who compared the two protocols for the Mimi Moto, average ISO CO ER (15 mg min<sup>-1</sup>) was 89 % lower than Champion et al. (2021), but our ISO PM<sub>2.5</sub> (2.6 mg min<sup>-1</sup>), OC (1.2 mg min<sup>-1</sup>), and EC (0.25 mg min<sup>-1</sup>) average ERs were 20 %, 530 %, and 45 % greater than Champion et al., 2021). One notable difference between these studies is that we used the medium combustion chamber during testing while Champion et al. (2020,2021) used the large chamber. Their tests therefore involved greater fuel loadings, which may have large impacts on CO emissions during shutdown, emphasizing the sensitivity of this protocol to stove configuration and power level definitions. Our baseline WBT average ERs for CO (11 mg  $min^{-1}$ ),  $PM_{2.5}$  (0.51 mg  $min^{-1}$ ), OC (0.40 mg  $min^{-1}$ ), and EC  $(0.14 \text{ mg min}^{-1})$  were 86 % less, 78 % less, 120 % greater, and 52 % less than Champion et al. (2021).

Generally, emissions from the different approaches presented here are substantially lower than previous gasifier stove lab studies; however, these studies used different types of gasifier stoves, such as the Philips fan stove (Bilsback et al., 2019), ACE 1 (Jathar et al., 2020), StoveTec TLUD (Jetter et al., 2012), or built their own (Shan et al., 2017). For example, our CO, PM<sub>2.5</sub>, OC, and EC ERs are 66 %, 91 %, 89 %, and 93 % lower than those reported by Bilsback et al. (2019). Similarly, CO and  $PM_{2.5}\ EF_ds$  are 89 % and 91 % lower than previous studies (Carter et al., 2014; Shan et al., 2017). However, these gasifier studies conducted tests under different testing protocols, such as the Firepower Sweep Test and WBT, and are not directly comparable to our approaches. When comparing approach-specific emissions, our Startup CO and PM $_{2.5}$  ERs are 37 % and 70 % lower than startup ERs reported by Bilsback et al. (2018). Additionally, Fedak et al. (2018) reported kerosene as the highest emitting startup material, shifting the Mimi Moto from PM<sub>2.5</sub> Tier 4 to Tier 1; however, our results show

kerosene to be lower emitting and remain similar to a Tier 4 emitting stove, possibly because we used twice as much kerosene. For Shutdown approaches, average burn phase CO ER is 87 % lower than for the StoveTec TLUD prototype in Jetter et al. (2012), but average burnout phase CO ER is 29 % higher than Bilsback et al. (2018) and 140 % higher than Jetter et al. (2012). For Refuel approaches, average refuel phase CO ER (340 mg min<sup>-1</sup>) are 37 % lower than Bilsback et al. (2018) at 540 mg min<sup>-1</sup>. While Bilsback et al. (2018) generally report higher ERs, the overall trend is similar: highest emissions for refueling, followed by shutdown, then startup.

We measured PM<sub>2.5</sub> ERs similar to those measured in the field and lab for LPG stoves (Bilsback et al., 2019; Johnson et al., 2019; Shen et al., 2018). Our PM<sub>2.5</sub> ERs ranged from 0.16 to 4.5 mg min<sup>-1</sup>, while other lab studies reported LPG PM<sub>2.5</sub> ERs ranging from 0.11 to 0.54 mg min<sup>-1</sup> (Bilsback et al., 2019; Shen et al., 2018). Johnson et al. (2019) measured LPG emissions in Uganda and reported an average LPG PM<sub>2.5</sub> ER (1.5 mg min<sup>-1</sup>) similar to the average in our study (1.7 mg min<sup>-1</sup>).

When comparing particle number emissions, ERs and EF<sub>m</sub>s from this study are on the same orders of magnitude as previous studies of gasifier stoves (Bilsback et al., 2019; Jathar et al., 2020; Shen et al., 2017). Shen et al. (2017) measured low power ER average (3.7  $\pm$  $0.33 \times 10^{13}~\text{\# min}^{-1})$  consistent with our Baseline ERs (5.4  $\pm$  1.8  $\times$  $10^{13}~\text{\# min}^{-1}$ ) while ther high power hot start ER average (8.3  $\pm$  $1.7 \times 10^{13} \, \text{# min}^{-1}$ ) was most similar to our Refuel ERs ( $7.4 \pm 1.8 \times 1$  $10^{13}$  # min<sup>-1</sup>). Our ISO size distributions closely resemble those reported for gasifier stoves by Jathar et al. (2020) and Just et al. (2013), with a mode diameter of approximately 20 nm. Our Shutdown size distributions more closely resemble those reported by Shen et al. (2017), with a mode diameter below the measurement cutoff diameter (14 nm) and not captured, and few particles emitted larger than 100 nm. Jathar et al. (2020) noted both solid and gas fuels have significant emissions below 10 nm, reinforcing that a major portion of the distribution shown here was not captured due to our 15 nm cutoff diameter. Shen et al. (2017) measured similar size distributions for high and low power phases, consistent with our burnout phase distributions, while Just et al. (2013) found that increasing the fan speed shifted the distribution to smaller diameters. This latter observation could explain the bimodal distribution seen in the Shutdown-Off burn phase, where a lower flow rate through the chamber promotes particle growth. Shen et al. (2017) found a second mode for high power hot start (which is most akin to refuel phase) for several forced- and natural-draft gasifier stoves. Overall, comparisons with other results exhibit general consistency, suggesting that our results capture trends in emissions and that our findings with a specific stove and fuel combination can be translated.

#### Implications and recommendations

While the results reported here are specific to the Mimi Moto, an individual but quite popular top-lit forced-draft semi-gasifier stove, they are likely extendable to any top-lit forced-draft stove burning pellets. Of the three modified operation approaches studied here, refueling led to the largest emissions, followed by ignition with kindling and shutdown at maximum fan speed, reinforcing the importance of secondary air flow for air-fuel mixing and maintaining sufficient temperatures for complete combustion. However, lab test emissions were all lower than the highest levels seen in Champion and Grieshop (2019) and remained primarily in ISO Tiers 5 and 4, so these very high field emissions are likely due to malfunction of the stove, such as a dead battery. One possibility to decrease stove malfunction events is proper cookstove use education, which has been shown to increase long-term improved stove use, and in the case of the Mimi Moto, improve stove performance (Lindgren, 2020; Seguin et al., 2018).

 Finding: Refueling with pellet char led to higher and more variable emissions than other approaches.

- Recommendation: Maintaining secondary air flow is essential for forced-draft cookstoves.
- Finding: Lab test emissions were all lower than the highest levels seen in Champion and Grieshop (2019).
- Recommendation: Proper cookstove use training including recommendations from this study, maintenance, and upkeep of stoves is the key for preventing high emission events in field settings.

When comparing our results to similar studies conducted with the Mimi Moto and ISO protocol, we find large relative emissions differences; thus, small operational differences can have large emissions implications. Our testing shows that these stoves can be nearly as clean as LPG and are at the limits of our ability to measure as concentrations approach measurement detection limits.

- Finding: Testing is very sensitive to subtle differences in protocol.
- Recommendation: Testing needs to be tightly constrained to allow for comparisons of one factor at a time.
- Finding: We approach limits of detection for a number of measurements, particularly during shorter or "cleaner" tests.
- Recommendation: Consider longer tests, larger flows through filter trains for greater loading, and influence of background, particularly in field settings where background concentrations can be high.

Because stove users are most likely to be around their stoves during startup and refueling, these modified operation results have the greatest exposure implications. In addition to material used for startup, a longer ignition process leads to higher PM<sub>2.5</sub> exposures. It is best to empty charred pellets from the combustion chamber as soon as the flame is extinguished, but if more heat is needed and burnout is necessary, then the fan should be turned off and the stove placed outside or the room evacuated. Refueling with pellet char is discouraged, but if necessary, pellets should not be filled above secondary air holes and the stove should be placed outside for at least the first five minutes when emissions are highest. Additionally, Refuel-High had very tall flames right after refueling that are a potential burn hazard (Fig. S21).

- Finding: Both ignition material and duration influence PM<sub>2.5</sub> emissions and have large exposure implications.
- Recommendation: Using kerosene, decreasing ignition time, and placing the stove outside during burnout and refuel could decrease exposures.

In addition to changes in stove operation, changes in stove design and distribution can consistently help to reduce emissions. A built-in sensor to turn off the fan after the flame dies could both decrease burnout emissions and discourage burnout all together. Stove distribution companies could provide two chambers of each size to allow users to easily swap the used chamber with pellet char to a new chamber with new pellets mid-cooking, allowing the used chamber to cool before using again. Additionally, they could provide kerosene or other liquid fuels for startup to discourage ignition with kindling and pellet char. Lastly, distribution companies could give credit for char which would be doubly beneficial by 1) not burning char which decreases exposure, and 2) decreasing net climate impacts by sequestering carbon. These insights can be applied to Mimi Moto improvements, distribution, and education, but are also useful for other stove types and future developments.

To minimize emissions, we recommend using kerosene for ignition, turning the fan off when pellets are done burning and the flame has extinguished, and reigniting with fresh pellets instead of pellet char. Our study shows relatively minor changes in operation can have substantial impacts on performance. Improved training and maintenance are needed in real-world applications to decrease the frequency of these high-emission events, and tightly controlled testing and detection

limits remain challenges to fully understanding factors contributing to these events.

#### **Funding**

This work was supported by the National Science Foundation (award # 1743741) and Jacobs Engineering, Inc. through a JNETS scholarship award to Stephanie Parsons.

#### **Declaration of competing interest**

The authors declare that they have no known competing financial interests or personal relationships that could have appeared to influence the work reported in this paper.

### Acknowledgements

We thank Aart de Heer from Mimi Moto for feedback on study design. We thank Grieshop Atmosphere and Environment Lab (GAEL) members Aditya Sinha, Mohammad Maksimul Islam, and Emily Floess for their lab instrument assistance and aid with filter analysis.

#### Appendix A. Supplementary data

Supplementary data to this article can be found online at https://doi.org/10.1016/j.esd.2022.08.004.

#### References

- Anderson, P. S., Reed, T. B., & Wever, P. W. (2007). Micro-gasification: What it is and why it works. *Boiling Point*, 35–37.
- Armbruster, D. A., & Pry, T. (2008). Limit of blank, limit of detection and limit of quantitation. Clinical Biochemist Reviews, 29, S49–S52.
- Bell, M. L., Dominici, F., Ebisu, K., Zeger, S. L., & Samet, J. M. (2007). Spatial and temporal variation in PM2.5 chemical composition in the United States for health effects studies. *Environmental Health Perspectives*, 115, 989–995. https://doi.org/10.1289/ehp.9621.
- Bilsback, K. R., Dahlke, J., Fedak, K. M., Good, N., Hecobian, A., Herckes, P., L'Orange, C., Mehaffy, J., Sullivan, A., Tryner, J., Van Zyl, L., Walker, E. S., Zhou, Y., Pierce, J. R., Wilson, A., Peel, J. L., & Volckens, J. (2019). A laboratory assessment of 120 air pollutant emissions from biomass and fossil fuel cookstoves. Environmental Science & Technology, 53, 7114–7125. https://doi.org/10.1021/acs.est.8b07019.
- Bilsback, K. R., Eilenberg, S. R., Good, N., Heck, L., Johnson, M., Kodros, J. K., Lipsky, E. M., L'Orange, C., Pierce, J. R., Robinson, A. L., Subramanian, R., Tryner, J., Wilson, A., & Volckens, J. (2018). The Firepower Sweep Test: A novel approach to cookstove laboratory testing. *Indoor Air*, 28, 936–949. https://doi.org/10.1111/ina.12497.
- Bond, T. C., Doherty, S. J., Fahey, D. W., Forster, P. M., Berntsen, T., DeAngelo, B. J., Flanner, M. G., Ghan, S., Kärcher, B., Koch, D., Kinne, S., Kondo, Y., Quinn, P. K., Sarofim, M. C., Schultz, M. G., Schultz, M., Venkataraman, C., Zhang, H., Zhang, S., ... Zender, C. S. (2013). Bounding the role of black carbon in the climate system: A scientific assessment. *Journal of Geophysical Research Atmospheres*, 118, 5380–5552. https://doi.org/10.1002/jgrd.50171.
- Carter, E. M., Shan, M., Yang, X., Li, J., & Baumgartner, J. (2014). Pollutant emissions and energy efficiency of chinese gasifier cooking stoves and implications for future intervention studies. Environmental Science & Technology, 48, 6461–6467. https://doi.org/ 10.1021/es405723w.
- Caubel, J. J., Rapp, V. H., Chen, S. S., & Gadgil, A. J. (2020). Practical design considerations for secondary air injection in wood-burning cookstoves: An experimental study. *Development Engineering*, 5, Article 100049. https://doi.org/10.1016/j.deveng.2020. 100049
- Caubel, J. J., Rapp, V. H., Chen, S. S., & Gadgil, A. J. (2018). Optimization of secondary air injection in a wood-burning cookstove: An experimental study. *Environmental Science & Technology*, 52, 4449–4456. https://doi.org/10.1021/acs.est.7b05277.
- Champion, W. M., & Grieshop, A. P. (2019). Pellet-fed gasifier stoves approach gas-stove like performance during in-home use in Rwanda. *Environmental Science & Technology*, 53, 6570–6579. https://doi.org/10.1021/acs.est.9b00009.
- Champion, W. M., Hays, M. D., Williams, C., Virtaranta, L., Barnes, M., Preston, W., & Jetter, J. J. (2021). Cookstove emissions and performance evaluation using a new ISO protocol and comparison of results with previous test protocols. Environmental Science & Technology, 55, 15333–15342. https://doi.org/10.1021/acs.est.1c03390.
- Champion, W. M., Warren, S. H., Kooter, I. M., Preston, W., Krantz, Q. T., DeMarini, D. M., & Jetter, J. J. (2020). Mutagenicity- and pollutant-emission factors of pellet-fueled gasifier cookstoves: Comparison with other combustion sources. *The Science of the Total Environment*, 739, Article 139488. https://doi.org/10.1016/j.scitotenv.2020. 139488
- Chen, Y., Shen, G., Su, S., Du, W., Huangfu, Y., Liu, G., Wang, X., Xing, B., Smith, K. R., & Tao, S. (2016). Efficiencies and pollutant emissions from forced-draft biomass-pellet semi-

- gasifier stoves: Comparison of International and chinese water boiling test protocols. *Energy for Sustainable Development*, 32, 22–30. https://doi.org/10.1016/j.esd.2016.02.008.
- Clean Cooking Alliance (2014). The water boiling test Version 4.2.3.
- Colorado State University. (2015). Mimi\_Moto\_IWA-Tiers of performance WBT 4.2.3 report REV.A (IWA Tiers of Performance Report). Colorado State University, Colorado State University Advanced Biomass Cookstoves Lab.
- Eilenberg, S. R., Bilsback, K. R., Johnson, M., Kodros, J. K., Lipsky, E. M., Naluwagga, A., Fedak, K. M., Benka-Coker, M., Reynolds, B., Peel, J., Clark, M., Shan, M., Sambandam, S., L'Orange, C., Pierce, J. R., Subramanian, R., Volckens, J., & Robinson, A. L. (2018). Field measurements of solid-fuel cookstove emissions from uncontrolled cooking in China, Honduras, Uganda, and India. Atmospheric Environment, 190, 116–125. https://doi.org/10.1016/j.atmosenv.2018.06.041.
- Fedak, K. M., Good, N., Dahlke, J., Hecobian, A., Sullivan, A., Zhou, Y., Peel, J. L., & Volckens, J. (2018). Chemical composition and emissions factors for cookstove startup (ignition) materials. *Environmental Science & Technology*, 52, 9505–9513. https://doi.org/10. 1021/acs.est.8b02218.
- Garland, C., Delapena, S., Prasad, R., L'Orange, C., Alexander, D., & Johnson, M. (2017). Black carbon cookstove emissions: A field assessment of 19 stove/fuel combinations. *Atmospheric Environment*, 169, 140–149. https://doi.org/10.1016/j.atmosenv.2017.08.040.
- Grieshop, A. P., Marshall, J. D., & Kandlikar, M. (2011). Health and climate benefits of cookstove replacement options. Energy Policy, Clean Cooking Fuels and Technologies in Developing Economies, 39, 7530–7542. https://doi.org/10.1016/j.enpol.2011.03.024.
- Gutiérrez, J., Chica, E. L., & Pérez, J. F. (2022). Parametric analysis of a gasification-based cookstove as a function of biomass density, gasification behavior, airflow ratio, and design. ACS Omega, 7, 7481–7498. https://doi.org/10.1021/acsomega.1c05137.
- Health Effects Institute. (2020). State of global air 2020. A special report on global exposure to air pollution and its health impacts. Boston, MA.
- Hinds, W. C. (2012). Aerosol technology: Properties, behavior, and measurement of airborne particles (2nd ed.). John Wiley & Sons.
- IPCC (2021). Summary for policymakers. NoIn V. Masson-Delmotte, P. Zhai, A. Pirani, S. L. Connors, C. Péan, S. Berger, & B. Zhou (Eds.), Climate change 2021: The physical science basis. Contribution of Working Group I to the sixth assessment report of the intergovernmental panel on climate change. Cambridge University Press In Press.
- Islam, M. M., Wathore, R., Zerriffi, H., Marshall, J. D., Bailis, R., & Grieshop, A. P. (2020). Inuse emissions from biomass and LPG stoves measured during a large, multi-year cookstove intervention study in rural India. *The Science of the Total Environment*, 143698. https://doi.org/10.1016/j.scitotenv.2020.143698.
- ISO (2018a). ISO 19867-1: Clean cookstoves and clean cooking solutions Harmonized laboratory test protocols Part 1: Standard test sequences for emissions and performance, safety, and durability.
- ISO (2018b). ISO/TR 19867-3: Clean cookstoves and clean cooking solutions Harmonized laboratory test protocols — Part 3: Voluntary performance targets for cookstoves based on laboratory testing (No. ISO/TR 19867-3:2018(E)).
- Jathar, S. H., Sharma, N., Bilsback, K. R., Pierce, J. R., Vanhanen, J., Gordon, T. D., & Volckens, J. (2020). Emissions and radiative impacts of sub-10 nm particles from biofuel and fossil fuel cookstoves. Aerosol Science and Technology, 1–13. https://doi.org/10.1080/02786826.2020.1769837.
- Jetter, J. J., & Kariher, P. (2009). Solid-fuel household cook stoves: Characterization of performance and emissions. *Biomass and Bioenergy*, 33, 294–305. https://doi.org/10. 1016/j.biombioe.2008.05.014.
- Jetter, J. J., Zhao, Y., Smith, K. R., Khan, B., Yelverton, T., DeCarlo, P., & Hays, M. D. (2012). Pollutant emissions and energy efficiency under controlled conditions for household biomass cookstoves and implications for metrics useful in setting international test standards. Environmental Science & Technology, 46, 10827–10834. https://doi.org/10. 1021/es301693f.
- Johnson, M. A., Garland, C. R., Jagoe, K., Edwards, R., Ndemere, J., Weyant, C., Patel, A., Kithinji, J., Wasirwa, E., Nguyen, T., Khoi, D. D., Kay, E., Scott, P., Nguyen, R., Yagnaraman, M., Mitchell, J., Derby, E., Chiang, R. A., & Pennise, D. (2019). In-home emissions performance of cookstoves in Asia and Africa. *Atmosphere*, 10, 290. https://doi.org/10.3390/atmos10050290.
- Just, B., Rogak, S., & Kandlikar, M. (2013). Characterization of ultrafine particulate matter from traditional and improved biomass cookstoves. *Environmental Science & Technology*, 47, 3506–3512. https://doi.org/10.1021/es304351p.
- Kampa, M., & Castanas, E. (2008). Human health effects of air pollution. Environmental Pollution, 151, 362–367. https://doi.org/10.1016/j.envpol.2007.06.012 Proceedings of the 4th International Workshop on Biomonitoring of Atmospheric Pollution (With Emphasis on Trace Elements).
- Khalek, I. A., Kittelson, D. B., & Brear, F. (2000). Nanoparticle growth during dilution and cooling of diesel exhaust: Experimental investigation and theoretical assessment. https://doi.org/10.4271/2000-01-0515.
- Kirch, T., Birzer, C. H., Medwell, P. R., & Holden, L. (2016). The role of primary and secondary air on wood combustion in cookstoves. *International Journal of Sustainable Energy*, 37, 268–277. https://doi.org/10.1080/14786451.2016.1166110.
- Kirch, T., Medwell, P. R., & Birzer, C. H. (2016). Natural draft and forced primary air combustion properties of a top-lit up-draft research furnace. *Biomass and Bioenergy*, 91, 108–115. https://doi.org/10.1016/j.biombioe.2016.05.003.
- Lacey, F. G., Henze, D. K., Lee, C. J., van Donkelaar, A., & Martin, R. V. (2017). Transient climate and ambient health impacts due to national solid fuel cookstove emissions. Proceedings of the National Academy of Sciences, 114, 1269–1274. https://doi.org/10.1073/pnas.1612430114.
- Li, N., Sioutas, C., Cho, A., Schmitz, D., Misra, C., Sempf, J., Wang, M., Oberley, T., Froines, J., & Nel, A. (2003). Ultrafine particulate pollutants induce oxidative stress and mitochondrial damage. *Environmental Health Perspectives*, 111, 455–460. https://doi.org/ 10.1289/ehp.6000.

- Li, Q., Jiang, J., Qi, J., Deng, J., Yang, D., Wu, J., Duan, L., & Hao, J. (2016). Improving the energy efficiency of stoves to reduce pollutant emissions from household solid fuel combustion in China. Environmental Science & Technology Letters, 3, 369–374. https://doi.org/10.1021/acs.estlett.6b00324.
- Lindgren, S. A. (2020). Clean cooking for all? A critical review of behavior, stakeholder engagement, and adoption for the global diffusion of improved cookstoves. *Energy Research and Social Science*, 68, Article 101539. https://doi.org/10.1016/j.erss.2020. 101539
- Lobscheid, A., Fitts, G., Lodoysamba, S., Maddelena, R., & Dale, L. (2012). Pilot study of fuel and stove use behavior of mongolian ger households (no. LBNL-6543E). Berkeley, CA (United States): Lawrence Berkeley National Lab. (LBNL). https://doi.org/10.2172/ 1165075.
- Maddalena, R. L., Lunden, M. M., Wilson, D. L., Ceballos, C., Kirchstetter, T. W., Slack, J. L., & Dale, L. L. (2014). Quantifying space heating stove emissions related to different use patterns in Mongolia. *Energy and Environment Research*, 4, Article p147. https://doi.org/10.5539/eer.v4n3p147.
- Meyer, L., Brinkman, S., van Kesteren, L., Leprince-Ringuet, N., & van Boxmeer, F. (2015). Technical support unit for the synthesis report (pp. 169).
- Mimi Moto (2021). Mimi Moto Clean cooking for all. URLhttps://mimimoto.nl/ (Accessed 1 December 2021).
- Mukunda, H. S., Dasappa, S., Paul, P. J., Rajan, N. K. S., Yagnaraman, M., Kumar, D. R., & Deogaonkar, M. (2010). Gasifier stoves science, technology and field outreach. *Current Science*, 98, 12.
- Peters, A., Wichmann, H. E., Tuch, T., Heinrich, J., & Heyder, J. (1997). Respiratory effects are associated with the number of ultrafine particles. *American Journal of Respiratory and Critical Care Medicine*, 155, 1376–1383. https://doi.org/10.1164/ajrccm.155.4. 9105082.
- Preble, C. V., Hadley, O. L., Gadgil, A. J., & Kirchstetter, T. W. (2014). Emissions and climate-relevant optical properties of pollutants emitted from a three-stone fire and the Berkeley-Darfur stove tested under laboratory conditions. *Environmental Science & Technology*, 48, 6484–6491. https://doi.org/10.1021/es5002715.
- Puzzolo, E., Zerriffi, H., Carter, E., Clemens, H., Stokes, H., Jagger, P., Rosenthal, J., & Petach, H. (2019). Supply considerations for scaling up clean cooking fuels for household energy in low- and middle-income countries. *GeoHealth*, 3, 370–390. https://doi.org/10.1029/2019GH000208.
- Ramanathan, V., Crutzen, P. J., Kiehl, J. T., & Rosenfeld, D. (2001). Aerosols, climate, and the hydrological cycle. *Science*, 294, 2119–2124. https://doi.org/10.1126/science. 1064034.
- Raub, J. A., & Benignus, V. A. (2002). Carbon monoxide and the nervous system. Neuroscience and Biobehavioral Reviews, 26, 925–940. https://doi.org/10.1016/s0149-7634(03)00002-2.
- Reece, S. M., Sinha, A., & Grieshop, A. P. (2017). Primary and photochemically aged aerosol emissions from biomass cookstoves: Chemical and physical characterization. *Environmental Science & Technology*, 51, 9379–9390. https://doi.org/10.1021/acs.est. 7b01881
- Reed, T. B., & Larson, R. (1996). A wood-gas stove for developing countries. Energy for Sustainable Development, 3, 34–37. https://doi.org/10.1016/S0973-0826(08)60589-X.
- Rehfuess, E., Mehta, S., & Prüss-Üstün, A. (2006). Assessing household solid fuel use: Multiple implications for the millennium development goals. *Environmental Health Perspectives*, 114, 373–378. https://doi.org/10.1289/ehp.8603.
- Roden, C. A., Bond, T. C., Conway, S., & Pinel, A. B. O. (2006). Emission factors and real-time optical properties of particles emitted from traditional wood burning cookstoves. Environmental Science & Technology, 40, 6750–6757. https://doi.org/10.1021/es052080i.
- Rosenthal, J. (2015). The real challenge for cookstoves and health: More evidence. *EcoHealth*, 12, 8–11. https://doi.org/10.1007/s10393-014-0997-9.
- Sandro, N., Agis, P., Gojmir, R., Vlasta, Z., & Müslüm, A. (2019). Using pellet fuels for residential heating: A field study on its efficiency and the users' satisfaction. *Energy and Buildings*, 184, 193–204. https://doi.org/10.1016/j.enbuild.2018.12.007.
- Schraufnagel, D. E. (2020). The health effects of ultrafine particles. Experimental & Molecular Medicine, 52, 311–317. https://doi.org/10.1038/s12276-020-0403-3.
- Seguin, R., Flax, Valerie L., & Jagger, P. (2018). Barriers and facilitators to adoption and use of fuel pellets and improved cookstoves in urban Rwanda. *PLoS One*, 13, Article e0203775. https://doi.org/10.1371/journal.pone.0203775.
- Shan, M., Carter, E., Baumgartner, J., Deng, M., Clark, S., Schauer, J. J., Ezzati, M., Li, J., Fu, Y., & Yang, X. (2017). A user-centered, iterative engineering approach for advanced biomass cookstove design and development. *Environmental Research Letters*, 12, Article 095009. https://doi.org/10.1088/1748-9326/aa804f.
- Shen, G. (2016). Changes from traditional solid fuels to clean household energies Opportunities in emission reduction of primary PM2.5 from residential cookstoves in China. Biomass and Bioenergy, 86, 28–35. https://doi.org/10.1016/j. biombioe.2016.01.004.
- Shen, G., Gaddam, C. K., Ebersviller, S. M., Vander Wal, R. L., Williams, C., Faircloth, J. W., Jetter, J. J., & Hays, M. D. (2017). A laboratory comparison of emission factors, number size distributions, and morphology of ultrafine particles from 11 different household cookstove-fuel systems. Environmental Science & Technology, 51, 6522–6532. https:// doi.org/10.1021/acs.est.6b05928.
- Shen, G., Hays, M. D., Smith, K. R., Williams, C., Faircloth, J. W., & Jetter, J. J. (2018). Evaluating the performance of household liquefied petroleum gas cookstoves. Environmental Science & Technology, 52, 904–915. https://doi.org/10.1021/acs.est. 7305155
- Shen, G., Tao, S., Wei, S., Zhang, Y., Wang, R., Wang, B., Li, W., Shen, H., Huang, Y., Chen, Y., Chen, H., Yang, Y., Wang, W., Wei, W., Wang, Xilong, Liu, W., Wang, Xuejun, & Simonich, S. L. M. (2012). Reductions in emissions of carbonaceous particulate matter and polycyclic aromatic hydrocarbons from combustion of biomass pellets in

- comparison with raw fuel burning. Environmental Science & Technology, 46, 6409–6416. https://doi.org/10.1021/es300369d.
- Smith, K. R., Bruce, N., Balakrishnan, K., Adair-Rohani, H., Balmes, J., Chafe, Z., Dherani, M., Hosgood, H. D., Mehta, S., Pope, D., & Rehfuess, E. (2014). Millions dead: How do we know and what does it mean? Methods used in the comparative risk assessment of household air pollution. *Annual Review of Public Health*, 35, 185–206. https://doi.org/10.1146/annurev-publhealth-032013-182356.
- Smith, K. R., Khalil, M. A. K., Rasmussen, R. A., Thorneloe, S. A., Manegdeg, F., & Apte, M. (1993). Greenhouse gases from biomass and fossil fuel stoves in developing countries: A Manila pilot study. *Chemosphere*, 26, 479–505. https://doi.org/10.1016/0045-6535(93)90440-G.
- Smith, K. R., Mehta, S., & Maeusezahl-feuz, M. (2004). Indoor air pollution from household use of solid fuels. Comparative Quantification of Health Risks, 18, 1435–1492.
- Tryner, J., Tillotson, J. W., Baumgardner, M. E., Mohr, J. T., DeFoort, M. W., & Marchese, A. J. (2016). The effects of air flow rates, secondary air inlet geometry, fuel type, and operating mode on the performance of gasifier cookstoves. *Environmental Science & Technology*, 50, 9754–9763. https://doi.org/10.1021/acs.est.6b00440.
- Tryner, J., Willson, B. D., & Marchese, A. J. (2014). The effects of fuel type and stove design on emissions and efficiency of natural-draft semi-gasifier biomass cookstoves. *Energy* for Sustainable Development, 23, 99–109. https://doi.org/10.1016/j.esd.2014.07.009.
- Turns, S. R. (2012). An introduction to combustion: Concepts and applications (3rd ed.). McGraw-Hill.
- US Department of Health and Human Services. (2012). Toxicological profile for carbon monoxide. Atlanta (GA): Agency for Toxic Substances and Disease Registry.

- US EPA (2019). Integrated Science Assessment (ISA) for particulate matter (final report, Dec 2019) (No. EPA/600/R-19/188). Washington, DC: U.S. Environmental Protection Agency.
- Varunkumar, S., Rajan, N. K. S., & Mukunda, H. S. (2011). Single particle and packed bed combustion in modern gasifier stoves—density effects. *Combustion Science and Technology*, 183, 1147–1163. https://doi.org/10.1080/00102202.2011.576658.
- Vu, T. V., Delgado-Saborit, J. M., & Harrison, R. M. (2015). Review: Particle number size distributions from seven major sources and implications for source apportionment studies. Atmospheric Environment, 122, 114–132. https://doi.org/10.1016/j.atmosenv. 2015.09.027.
- Wathore, R., Mortimer, K., & Grieshop, A. P. (2017). In-use emissions and estimated impacts of traditional, natural- and forced-draft cookstoves in rural Malawi. *Environmental Science & Technology*, 51, 1929–1938. https://doi.org/10.1021/acs.est.6b05557.
- Weyant, C. L., Thompson, R., Lam, N. L., Upadhyay, B., Shrestha, P., Maharjan, S., Rai, K., Adhikari, C., Fox, M. C., & Pokhrel, A. K. (2019). In-field emission measurements from biogas and Liquified Petroleum Gas (LPG) stoves. *Atmosphere*, 10, 729. https://doi.org/10.3390/atmos10120729.
- Wilbur, S., Williams, M., Williams, R., Scinicariello, F., Klotzbach, J. M., Diamond, G. L., & Citra, M. (2012). Toxicological profile for carbon monoxide, Agency for Toxic Substances and Disease Registry (ATSDR) toxicological profiles. Atlanta (GA): Agency for Toxic Substances and Disease Registry (US).
- Zhou, Y., Zhang, Z., Zhang, Y., Wang, Y., Yu, Y., Ji, F., Ahmad, R., & Dong, R. (2016). A comprehensive review on densified solid biofuel industry in China. *Renewable and Sustainable Energy Reviews*, 54, 1412–1428. https://doi.org/10.1016/j.rser.2015.09.096.